Journal of Hazardous Materials 424 (2022) 127363

Contents lists available at ScienceDirect

Journal of Hazardous Materials

journal homepage: www.elsevier.com/locate/jhazmat

Research paper

Size dependent impacts of a model microplastic on nitrification induced by interaction with nitrifying bacteria

Jongkeun Lee [a,b,1], Seulki Jeong [a,c,*,1], Chenghua Long [a], Kartik Chandran [a,**]

[a] Department of Earth and Environmental Engineering, Columbia University in the City of New York, 500 West 120th Street, New York, NY 10027, USA
[b] Department of Civil and Environmental Engineering, College of Engineering, Konkuk University, 120 Neungdong-ro, Gwangjin-gu, Seoul 05029, South Korea
[c] Seoul center, Korea Basic Science Institute, 6-7, Inchon-ro 22-gil, Seongbuk-gu, Seoul 02855, South Korea

ARTICLE INFO

Editor: Dr Shaily Mahendra

Keywords:
Microplastic
Polystyrene
Nitrification
Nitrifying bacteria
amoA expression

ABSTRACT

Two sizes of polystyrene (PS) were compared to investigate their impact on nitrification. The smaller PS (50 nm) had a higher impact than the larger PS (500 nm). Lower NO_2^- and NO_3^- accumulation was observed in the 50 nm PS treatment. There was no significant difference in DIN concentration between the control and 500 nm PS treatments. PS treatment did not have a significant influence on the specific ammonia oxidation rate, but the specific nitrite utilization rate was the lowest in the 50 nm PS treatment. The changes in transcript levels of *amoA* gene did not correspond well with the observed changes in DIN concentrations, suggesting that the effects of 50 nm PS treatment might be unrelated to biological phenomena, for which an actual uptake of PS is needed. The fluorescent images revealed that the smaller PS can easily access bacterial cells, which corroborated the results of inhibition of nitrification by the smaller PS. Notably, most of the PS particles did not penetrate bacterial cells, suggesting that the observed effects of 50 nm PS on nitrification might be due to disruption of the membrane potential of the cells.

1. Introduction

Microplastics (MPs), which are smaller than 5 mm (Law and Thompson, 2014), have become an emerging concern, and great attention is being paid to their toxic effects on ecosystems (Anbumani and Kakkar, 2018). MPs can produce smaller-sized particles by biological, photodegradation, and mechanical degradation (Cole et al., 2013). The physicochemical properties of MPs, such as size and surface charge, are significant parameters for their accumulation and toxicity, and affect organisms differently. In particular, as the particle size decreases from micro- to nano-, the impact on biological systems increases as small-sized particles are easily available to various organisms for uptake or transfer (Lehtiniemi et al., 2018; Lee et al., 2019). Numerous studies have reported the impact of MPs on marine environment organisms, such as zooplankton (Cole et al., 2013), shrimp (Gray and Weinstein, 2017), and zebrafish (Batel et al., 2016). The influence of different MPs (i.e., different sizes, polymer types, and shapes) on organisms from other ecosystems, excluding marine environments, is worth further exploration.

Various types of MPs have recently been detected in the inlets and outlets of municipal wastewater treatment plants (WWTPs) (Li et al., 2019, 2020; Sun et al., 2019). As MPs are capable of adsorbing toxicants owing to their high surface area (Wang et al., 2016), and contain additives such as polybromodiphenyl ethers (PBDEs) and phthalate esters (PAEs) (Cole et al., 2011), they can affect biological processes in WWTPs. Although MPs are potential new contaminants in the environment, their impact on wastewater treatment processes has rarely been reported and remains unclear. Nitrification, the oxidative conversion of ammonia to nitrite or nitrate by ammonia-oxidizing bacteria (AOB) and nitrite-oxidizing bacteria (NOB), is the first and limiting step in biological nitrogen removal (BNR) in wastewater treatment (Kapoor et al., 2016; Kim et al., 2006). As nitrifying bacteria are typically sensitive to environmental disruptions such as toxicants, including MPs (Kim et al., 2008), it is important to understand their effects on nitrification. Several studies have recently reported that MPs can potentially inhibit the nitrifying activities of AOB and NOB. Li et al. (2020) found that the

* Corresponding author at: Seoul center, Korea Basic Science Institute, 6-7, Inchon-ro 22-gil, Seongbuk-gu, Seoul, 02855, Korea
** Corresponding author at: Department of Earth and Environmental Engineering, Columbia University in the City of New York, 500 West 120th Street, New York, NY 10027, USA.
E-mail addresses: sjeong85@kbsi.re.kr (S. Jeong), kc2288@columbia.edu (K. Chandran).
[1] These authors contributed equally to this work. Author order was determined alphabetically.

https://doi.org/10.1016/j.jhazmat.2021.127363
Received 15 June 2021; Received in revised form 23 September 2021; Accepted 25 September 2021
Available online 28 September 2021

activated sludge nitrification and denitrification processes were affected by the addition of MPs such as polyester (PES), polyethylene (PE), polypropylene (PP), polystyrene (PS), and polyvinyl chloride (PVC) with an abundance of 1000–10,000 particles/L, and concluded that MPs in WWTPs need to be investigated. Sun et al. (2018) investigated the effect of PS on the inorganic nitrogen conversion efficiency of *Halomonas alkaliphila*. However, Liu et al. (2019) found that PES, PE, and PVC particles between 100 and 1200 μm and 50–10,000 particles/L density did not significantly affect the activities of AOB and NOB. Based on previous studies, the impact of MPs on nitrification is irregular and limited, and the type, size, shape, concentration, and physicochemical characteristics (e.g., surface charge and/or additives) of MPs could be the key determinants of their impacts on nitrification. Therefore, further studies are required.

The primary objective of this study was to explore the impact of different sizes of MPs on nitrification. PS, which is used for a wide range of applications (Rocha-Santos and Duarte, 2015), has a large annual production (>17 Mt) (Lithner et al., 2011), and is one of the most frequently detected MPs in WWTPs, was selected for this study. In general, microplastics usually refer to particles with sizes of > 100 nm or < 5 mm, and they are fragmented into smaller particles of < 100 nm, termed nanoplastics (Nguyen et al., 2019). Two sizes of PS, 50 nm and 500 nm that corresponding to nanoplastics and microplastics, were compared. Fluorescence images were obtained to investigate the interactions between PS and nitrifying bacteria. The transcriptional response of ammonia monooxygenase subunit A (*amoA*) exposed to PS was also evaluated to examine the sub-cellular responses of ammonia-oxidizing bacteria to PS exposure.

2. Materials and methods

2.1. Cell cultivation

The cells were cultured in a laboratory located at Columbia University in the City of New York for several years (Su et al., 2019). The cells were cultivated in a lab-scale nitrification sequencing batch reactor (SBR) with a working volume of 8 L. The bioreactors were initially seeded with activated sludge and fed with a nutrient medium containing 500 mg N/L ammonium and without any organic carbon source, to enrich for test cultures of nitrifying bacteria. The feed contained 500 mg/L NH_4^+-N and the following compounds (per liter): 0.102 g of KH_2PO_4, 0.261 g of $K_2HPO_4 \cdot 3H_2O$, 0.701 g of $NaHCO_3$, and 1 mL of trace element solution. The trace element solution contained the following (per liter): 3.336 g of $FeSO_4 \cdot 7H_2O$, 3.380 g of $MnSO_4 \cdot H_2O$, 0.673 g of $(NH_4)_6Mo_7O_{24} \cdot 4H_2O$, 0.833 g of $CuCl_2 \cdot 7H_2O$, 2.980 g of $ZnSO_4 \cdot 7H_2O$, and 0.567 g of $NiSO_4 \cdot 6H_2O$. The conditions of the SBR are listed in Table 1. The SBR was operated at a hydraulic retention time (HRT) of 1 d, utilizing four cycles per day with each cycle consisting of a 225 min feed and mixing period, 75 min reaction period, 30 min settling period, and 30 min decantation period. The reactor was mechanically mixed using a magnetic stirrer and aerated at a rate of 3 L/min at room temperature (22 ± 2 °C). The reactor pH was controlled automatically at 7.5 ± 0.10, using a 1.0 M sodium bicarbonate solution. Biomass samples were collected from the SBR during the reaction period and washed three times using SBR feed without NH_4^+. After each wash, the cells were centrifuged at 4000 *g* at 4 °C for 5 min. The washed cells were suspended in the SBR feed without NH_4^+ and stored at − 80 °C for subsequent analysis.

Table 1
The operating conditions of sequencing batch reactor (SBR) used in this study.

Conditions	Unit	Values	
Volume (V)	L	8	
Hydraulic retention time (HRT)	day	1	
Operation cycle	–	fill;	225 min
		reaction; settle;	75 min
		decant;	30 min
			30 min
Nitrogen loading	mg/L	500	
pH	–	7.5 ± 0.10	
Temperature	°C	22 ± 2	
DO	mg/L	3–4	

2.2. Polystyrene preparation

Fluorescent-labeled and non-functionalized PS were purchased with nominal diameters of 50 nm and 500 nm from Polyscience Inc. (USA). PS exhibited excitation and emission peaks at 441/486 nm. The concentrations were 2.6% and 2.7% solid suspension for 50 nm and 500 nm, respectively, and the suspending medium was DI water. The density of the two PS was ~ 1.05 g/cm^3, similar to the cell densities. The stock solution of PS was serially diluted with ultra-pure water, and an appropriate volume of each solution was added to a concentration of 300 mg PS/L for the exposure experiment. The exposure concentration was determined to be high enough to examine the impact of PS on nitrifying bacteria based on previous studies (Rehse et al., 2016; Gerdes et al., 2019; Hierl et al., 2021). The hydrodynamic diameter and zeta potential values of PS in the medium used in this study were measured using a particle analyzer (Zetasizer, Malvern Instruments Ltd, UK).

2.3. Experimental setup

2.3.1. Polystyrene exposure experiment

Batch exposure experiments were conducted to investigate the effects of PS on nitrification, which is mediated by AOB and NOB. An NH_4^+-N (500 mg/L) solution was added to 80 mL of the cultivated cells in a medium using ammonium sulfate ($(NH_4)_2SO_4$) and then exposed to two different sizes of PS, 50 nm and 500 nm. Control cells in the medium were exposed to 500 mg/L NH_4^+-N only. Continuous air supply was provided to all the cells and pH was maintained at 7.0 ± 0.5 using 0.5 M sodium hydroxide (NaOH) during the experiment. The cell suspensions were collected at the beginning of each experiment (0 h) and after 2, 4, and 8 h. The effects of PS on the nitrifying bacteria were investigated by measuring the concentrations of dissolved inorganic nitrogen (DIN), ammonia (NH_4), nitrite (NO_2), and nitrate (NO_3).

2.3.2. Chemical Measurements

The chemical oxygen demand (tCOD) was measured at 0 h using a high range of digestion solution for 20–1500 mg/L COD (Hach Company, USA), and was used to normalize the specific NH_4 oxidation and NO_2 utilization rates. The DIN (NH_4, NO_2, and NO_3) concentrations were determined at each sampling time. NH_4^+ was measured using a standard ammonia ion-selective electrode (Thermo Fisher Scientific, USA). Dionex ICS-2100 ion chromatography using a Dionex IonPac AS-18 IC column (Thermo Fisher Scientific, USA) was used to determine NO_3 and NO_2 concentrations. The fluorescent PS in collected samples at 8 h was observed using a spinning disk confocal microscope (Nikon Ti Eclipse inverted, Nikon Corporation, Tokyo, Japan) equipped with a fluorescent filter, at the Columbia University Irving Medical Center (New York, NY, USA). Fluorescent images were compiled using the NIS-Elements software. For quantification of the functional gene expression of *amoA* at each sampling time, the collected cells were treated with RNAprotect Bacteria Reagent (Qiagen, USA) following the manufacturer's instructions and stored at −80 °C until DNA and RNA extraction. DNA was extracted from the collected cells using the QIAamp DNA Mini Kit (Qiagen, USA), and the extracted DNA was stored at −20 °C. Total RNA was extracted from the collected cells using the RNeasy Mini Kit (Qiagen, USA), and the extracted RNA was stored at −80 °C. The quantity and quality of DNA and RNA were measured using a NanoDrop Lite UV spectrophotometer (Thermo Scientific, USA). cDNA was synthesized from total RNA using the QuantiTect Reverse Transcription Kit (Qiagen, USA) following the manufacturer's protocol. *amoA* expression in DNA and cDNA was quantified in triplicate using quantitative polymerase

chain reaction (qPCR) assays with a CFX384 Touch Real-Time PCR Detection System (Bio-Rad, USA) using the primers *amoA*-1 F (5′-GGGGTTTCTACTGGTGGT) and *amoA*-2R (5′- CCCCTCKGSAAAG CCTTCTTC) (Rotthauwe et al., 1997). qPCR reactions were conducted in a solution containing 12.5 μL of 2 × iQ SYBR Green Supermix (Bio-Rad, USA), 1 μL of forward and reverse primers (5 μmol/L), 9.5 μL of DNA-grade deionized distilled water (Fisher Scientific, USA), and 1 μL of DNA or cDNA. Standard curves for qPCR were generated via serial decimal dilutions of plasmid DNA containing the *amoA* gene insert. Thermal cycling was conducted with an initial denaturation step at 94 °C for 2 min, which was followed by 40 cycles of denaturation at 94 °C for 30 s, primer annealing at 57 °C for 40 s, and elongation at 72 °C for 30 s. Melt curve analysis was conducted from 50° to 95 °C with 0.5 °C increments, each for 10 s. The absence of primer dimers was confirmed by a melt curve analysis (data not shown).

2.4. Calculation and statistical analysis

The following equations were used to estimate the rates of nitrification, specific ammonia oxidation rate, and specific nitrite utilization rate (mg-N/g-VSS•d).

$$\text{specific ammonia oxidiation rate} = \frac{C_{NH_4,t_1} - C_{NH_4,t_2}}{\Delta t \bullet X} \quad (1)$$

$$\text{specific nitrite utilization rate} = \frac{C_{NO_2,t_1} - C_{NO_2,t_2}}{\Delta t \bullet X} \quad (2)$$

where C_{NH4} and C_{NO2} indicate the concentrations of ammonia and nitrite after time t_1 and t_2, respectively (mg-N/L). Δt represents the difference between the end time and the initial time of measurement (d), and X is the concentration of biomass (gVSS/L). The conversion factor used between CODx and VSS was 1.42 CODx/g-VSS (Ahn et al., 2008).

The *amoA* gene expression in cDNA was normalized to the *amoA* gene expression in DNA to calculate the relative gene expression, using Eq. (3).

$$\text{Relative gene expression} = \frac{amoA \text{ concentration in cDNA (copies/mL)}}{amoA \text{ concentration in DNA (copies/mL)}} \quad (3)$$

All data obtained from this study were expressed as the mean ± standard deviation (S.D.), and the significance was determined using a one-way analysis of variance (one-way ANOVA) test to compare the differences between the control and exposed groups using Microsoft Excel. The significance level was set at $P < 0.05$.

3. Results

3.1. Effects of polystyrene on nitrification

The DIN concentrations, NH_4^+, NO_2^-, and NO_3^- during nitrification when exposed to PS are shown in Fig. 1. All samples showed similar trends with increasing NO_2^- and NO_3^- concentrations and decreasing NH_4^+ concentrations with time. The lowest NO_2^- and NO_3^- concentrations were observed in the 50 nm PS treatment after 8 h ($P < 0.05$). Most notably, higher NO_2^- accumulation was observed in both PS treatments than in the control at 4 h. The specific ammonia oxidation rate and nitrite accumulation utilization rate, which exhibited the potential AOB and NOB activities, respectively, were calculated and are listed in Table 2. The overall specific ammonia oxidation rates at 8 h in the control, 50 nm PS, and 500 nm PS treatments were 1325 ± 77.5, 1301 ± 55.5, and 1512 ± 8.77 mg-N/g-VSS•d, respectively, suggesting that PS treatment had no significant impact on the oxidation rate of ammonia to nitrite, which was stimulated only when exposed to 500 nm PS. This was corroborated by the high NO_2^- and low NH_4^+ concentrations in the 500 nm PS treatment. The overall specific nitrite utilization rates were 1045 ± 37.4, 856 ± 65.2, and 1074 ± 25.9 mg-N/g-VSS•d for control, 50 nm PS, and 500 nm PS treatment, respectively. This corresponded with the lowest concentrations of NO_3^- in the 50 nm PS treatment. Interestingly, the effect of PS treatment on nitrification was dependent on exposure time. The specific ammonia oxidation rate seemed to be stimulated by both PS treatments for the first 2 h when compared to the control, and then decreased up to 4 h. After 8 h, there was no significant difference in the specific ammonia oxidation rate between the control and 50 nm PS treatments, whereas it was still stimulated in the 500 nm PS treatment. For the specific nitrite utilization rate, a relatively constant rate was obtained in the control for 8 h. When exposed to PS, the specific nitrite utilization rate increased for the first 2 h, similar to that of the specific ammonia oxidation rate, and then decreased until 4 h. However, the decrease in the specific nitrite utilization rate continued up to 8 h in the 50 nm PS treatment, whereas it recovered to a significantly similar rate to that of the control after 4 h in the 500 nm PS treatment ($P < 0.05$).

3.2. The responses of amoA in cells exposed to polystyrene

The relative changes in the *amoA* transcript levels in response to PS exposure during nitrification are shown in Fig. 2. The relative expression of *amoA* in all samples was similar during the initial 2 h period. Notably, a positive effect on the expression of *amoA* was observed in the PS treatment at 4 h. Thereafter, a statistically significant increase in *amoA* expression was found in the 50 nm PS treatment, whereas the levels of *amoA* expression in the 500 nm PS treatment were comparable to those in the control. Unexpectedly, although a slight inhibition of nitrification was observed in the 50 nm PS treatment, *amoA* expression in PS treatment did not correspond well with the changes in NH_4^+ concentrations. This inconsistency demonstrates that the inhibition by PS might be unrelated to biological phenomena, for which the actual uptake of PS is needed.

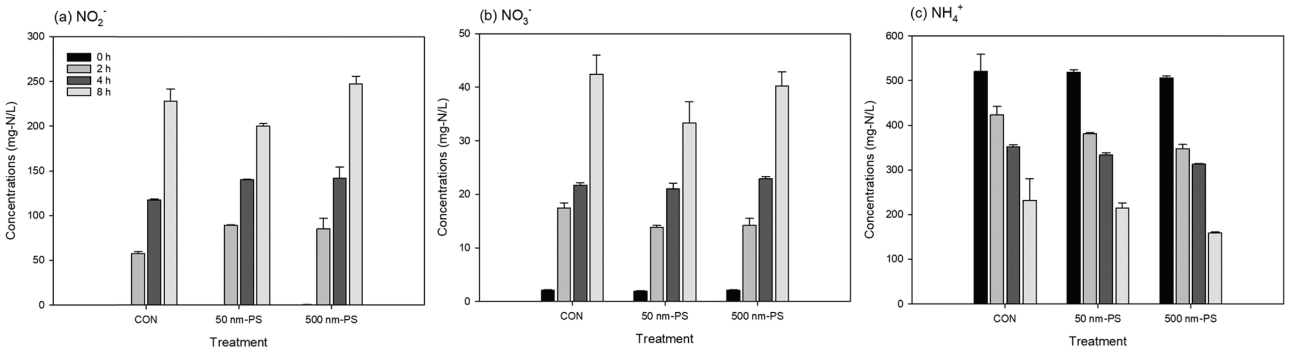

Fig. 1. Impacts of PS on the dissolved inorganic nitrogen concentrations, (a) NO_2^-, (b) NO_3^-, and (c) $NH_4^+$for 8 h.

Table 2
Changes in the specific ammonia oxidation rate and the specific nitrite utilization rate with PS treatment for 8 h.

PS treatment	Specific NH_4 oxidation rate (mg-N/g-VSS•d)				Specific NO_2 utilization rate (mg-N/g-VSS•d)			
	0–2 h	2–4 h	4–8 h	overall	0–2 h	2–4 h	4–8 h	overall
Control	1782 ± 308	1312 ± 238	1103 ± 428	1325 ± 77.5	1053 ± 57.1	1100 ± 11.7	1014 ± 109	1045 ± 37.4
50 nm-PS	2361 ± 277	804 ± 70.0	1020 ± 7.36	1301 ± 55.5	1520 ± 100	880 ± 40.0	512 ± 59.6	856 ± 65.2
500 nm-PS	2754 ± 210	606 ± 138	1344 ± 54.0	1512 ± 8.77	1484 ± 191	984 ± 2.61	920 ± 45.1	1074 ± 25.9

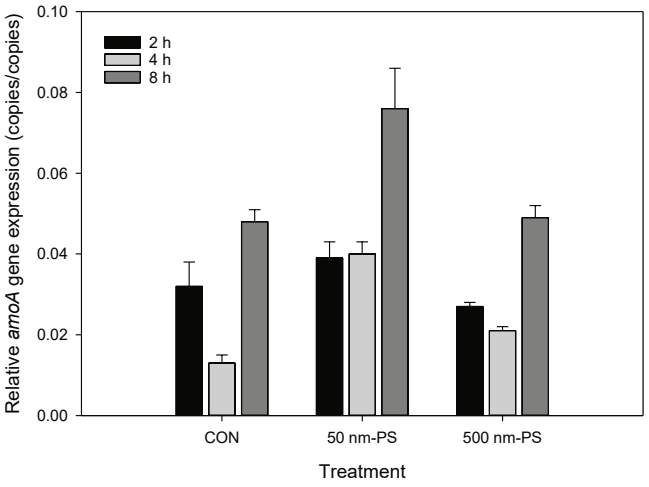

Fig. 2. Changes in the relative levels of *amoA* gene expression according to PS treatment with time.

3.3. The interaction between PS and nitrifying bacteria

The fluorescent images were investigated to determine the reason for the size-dependent effect of PS on bacterial flocs and to examine their interactions. Fig. 3 shows fluorescent images of 50 nm PS (a) and 500 nm PS (b) around the nitrifying bacteria. Fluorescent PS was clearly detected in both the treatments. A stronger fluorescence intensity was observed in the 50 nm PS treatment than that in the 500 nm PS treatment, implying that the smaller PS can easily interact with the nitrifying bacteria, and consequently, is likely to affect nitrification. This corresponded well with our results that inhibition by PS was only observed in the 50 nm PS treatment. The most interesting finding was that the fluorescence was predominantly observed in the space between bacterial flocs and surrounding bacteria, indicating that the inside of the bacterial cells was empty, as indicated by the white arrows in Fig. 3. This revealed that most of the PS particles did not penetrate the bacterial cells. This could be a result of the surface charge of the PS used in this study. The zeta potential values of the PS were negative (approximately –31.8 ± 2.57 for 50 nm PS and –41.4 ± 1.52 for 500 nm PS), as shown in Table 3. PS were slightly negatively charged as a result of surface charges, which arise from fragments of the initiator used to start the polymerization reaction. (Lundqvist et al., 2008). There are several examples of studies using negative-charged PS (Hwang et al., 2020; Schabikowski et al., 2018; Kloet et al., 2015). As most bacterial cell walls generally have a net negative charge, the negatively charged PS would not be accessible to the bacterial cells. Thus, PS was mainly found outside the space of the bacterial cells in the present study. This finding suggests that the observed impacts of 50 nm PS on nitrification might be

Table 3
Zeta potential values of the PS used in this study.

Size (nm)	Concentration (mg/L)	Hydrodynamic diameter (nm)	Zeta potential (mV)
50	300	64.7 ± 0.74	-31.8 ± 2.57
500	300	483 ± 11.6	-41.4 ± 1.52

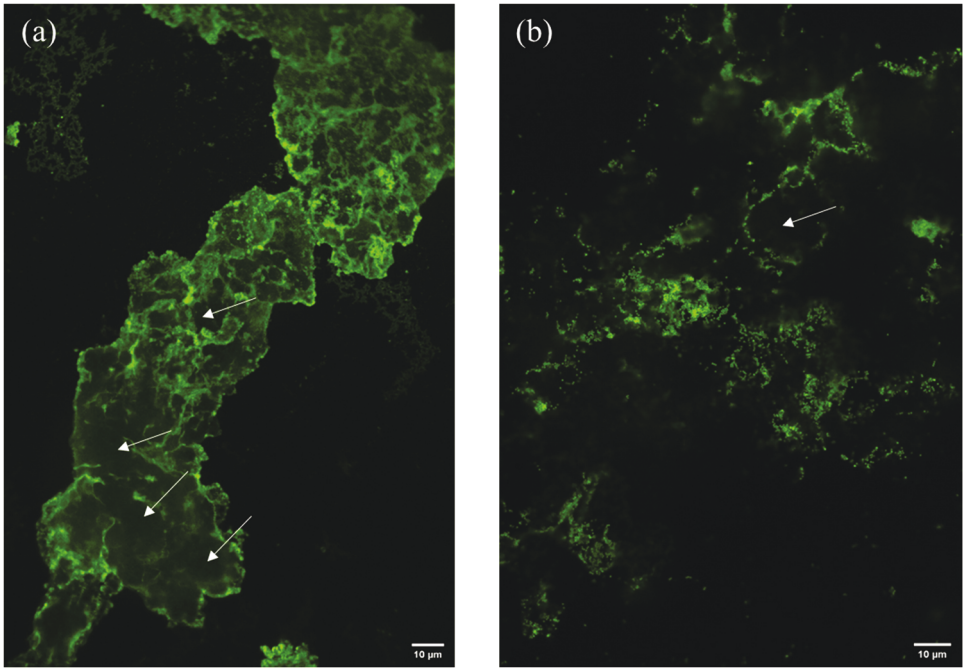

Fig. 3. Comparison of the presence of two different sizes of fluorescent PS around the nitrifying bacteria: (a) 50 nm PS treatment and (b) 500 nm PS treatment.

due to physical damage, such as disruption of the membrane potential of the cells. If so, the inconsistency between DIN concentration and the response of the *amoA* gene, which is a critical enzyme in nitrification, could be explained by the physical interaction between nitrifying bacteria and PS, and not by the uptake of PS by the bacteria. Several studies have suggested that negatively charged particles are likely to affect the cellular membrane and, subsequent biological effects (Moghadam et al., 2012; Jeon et al., 2018).

4. Discussion

Our study demonstrates that PS contamination affects nitrification, and its impact depends on PS size and exposure time. The changes in the DIN concentration, specific ammonia oxidation rate, and specific nitrite utilization rate showed that at smaller PS affected the overall nitrification process. The 50 nm PS inhibited the oxidation of NH_4^+ to NO_2^-, resulting in the lowest accumulation of NO_2^- ($P < 0.05$). However, they did not interfere with the specific ammonia oxidation rate at 8 h. In the case of the conversion of NO_2^- to NO_3^-, the production of NO_3^- and the specific nitrite utilization rate were significantly influenced by 50 nm PS at 8 h ($P < 0.05$). Interestingly, the impact of PS on nitrification differed with exposure time. PS treatment unexpectedly accelerated nitrification in the early stages, up to 4 h for NO_2^- accumulation, and 2 h for nitrification rate. Thereafter, their impact depended on the size of the PS. The impact of MPs on nitrification in previous studies was not significant. However, several studies have reported that MPs can affect nitrification. Wang et al. (2020) investigated the co-effects of four MPs, including 1 mg/L of PE, PS, PVC, and PA with triclosan on nitrification in lab-scale nitrifying SBRs. They found that no measurable inhibition was observed on nitrification in the PE- and PS-loaded reactors, but PVS and PA loading on reactors resulted in a rapid loss of nitrification function for 14 days. The study conducted by Li et al. (2020) stated that MPs with < 10,000 particle/L concentration in wastewater had low effects on nitrification until 3 h. The ammonia oxidation rate was reduced to 0.69, 0.55, and 0.49 times with PVC treatment compared with that of the control for 12 h (Song et al., 2020). He et al. (2021) investigated the effect of different concentrations (0.01, 0.05, and 0.1 g/L) and particle sizes of PS (0–75, 75–150, and 150–300 μm) on nitrogen removal in an activated sludge system. The results showed that the ammonia oxidation process was affected by the presence of PS at concentrations greater than 0.05 g/L. Surprisingly, they stated that the higher particle size of PS results in a lower ammonia oxidation rate, which is contrary to the results obtained in our study. The effects of PS treatment on nitrification, irrespective of the outcome and the nitrifying step, remain unclear because of the inconsistencies in results obtained from different studies. Nevertheless, it is evident that MP contamination has potential impacts on nitrification, suggesting that MP contamination should be considered when investigating wastewater treatment processes. A long-term exposure experiment should be conducted to reveal the effects of MPs on nitrification.

No significant correlation between PS treatment and *amoA* gene expression was observed in this study. In the present study, the *amoA* gene might have decreased due to PS stress. *amoA,* a critical enzyme in oxidizing NH_4^+ to hydroxylamine (NH_2OH), could be a useful proxy for evaluating nitrification performance in the engineered nitrification process (Kim et al., 2016; Seeley et al., 2020). However, the response of *amoA* expression did not correspond well with the observed changes in NH_4^+ *concentrations*. PS treatment appeared to slightly enhance nitrification and NO_2^- accumulation, as evidenced by higher *amoA* gene expression relative to the control, during the first 4 h. However, the inconsistency, a sharp stimulation of the *amoA* gene in the 50 nm PS treatment after 4 h, could not be explained. This might indicate that PS treatment had no immediate acute effect on the functional gene expression of nitrifying bacteria. Few studies have evaluated the potential of MPs to influence *amoA* gene expression. In a study by Wang et al. (2020), the *amoA* gene was not significantly affected by MPs. They found that the activity of AOB was inhibited by PS loading for a brief period, but it could recover, and this corresponded well with the changes in *amoA* expression after 500 nm PS treatment. In contrast, several studies have reported that MPs may facilitate the activity of nitrifying communities. Seeley et al. (2020) observed that polyurethane foam (PUF) or polylactic acid (PLA) enhanced nitrification and correspondingly elevated *amoA* gene abundance over time. They presented the possibility of the contribution of labile inorganic N for nitrification by in situ degradation of PUF, as PUF contains N in the polymer backbone, unlike other polymers tested in their study. Romera-Castillo et al. (2018) found that plastics release dissolved organic carbon (DOC) into ambient seawater, stimulating the activity of microbes. However, they did not investigate changes in the expression of functional gene related to N cycling.

The results obtained from this study may provide insights into the mechanisms by which MPs influence the nitrification process. It is worth mentioning that a smaller PS could easily access nitrifying bacteria, but did not penetrate the cells. Although PS only exists outside of bacterial cells, the ecological impact of PS on nitrifying bacteria suggests that PS potentially causes physiological disruption in the cell membrane. Sun et al. (2018) and Fu et al. (2018) also found that MPs may interact with bacterial membranes, leading to stress on the cytoplasmic membrane. Rossi et al. (2014) found that PS significantly reduced molecular diffusion and softened the membrane, severely affecting the activity of membrane proteins and thereby cellular function. Since the surface charge of PS are depending on their surroundings, it could be a significant factor to interaction between PS and bacteria. Kim et al. (2006) also mentioned that positively charged MPs bind cells tightly due to electrostatic attraction, whereas negatively charged MPs bind cells loosely through van der Waals forces, acid-base interactions, and electrostatic forces. The evidence for the different binding affinities by surface charge of PS supports our findings. However, a few studies have been conducted on the toxicity caused by the release of substances from MPs, and no studies have focused on the physical adsorption of MPs to the cells. Our results highlighted that the impact of MPs is dependent on particle size and exposure time, and might result in physical disruption. This study is aware of the interactions between MPs and nitrifying bacteria. Further studies are needed to determine the detailed mechanisms of disruption to the membrane potential of the cells, as well as the increasing *amoA* gene expression by exposing MPs.

5. Conclusion

The size-dependent effects of PS on nitrifying bacteria that contribute to the nitrification process were examined. Although the lowest NO_2^- and NO_3^- production was observed in the 50 nm PS treatment, the nitrification process did not stop. The oxidation rate of ammonia to nitrite, the first nitrification process, did not change significantly, whereas the nitrite utilization rate, the second nitrification process for the conversion of nitrite to nitrate, was inhibited by exposure to 50 nm PS. The impact of PS depends on exposure time. The changes in *amoA* expression did not directly correlate with the changing trend of DIN concentrations in the present study, but was promoted by the 50 nm PS. It can be inferred that the impact of PS on nitrifying bacteria might be unrelated to biological phenomena corresponding to uptake or penetration of PS, as revealed by the fluorescent images, which showed that most of the PS existed outside of the bacterial cells. This study demonstrated that PS could interrupt nitrification. However, an accurate mechanism needs to be identified in further studies. Nevertheless, the findings of this study can contribute to the understanding of the potential influence of PS on nitrogen cycling in wastewater treatment.

CRediT authorship contribution statement

Jongkeun Lee: Writing – review & editing, experiment. **Seulki Jeong**: Writing – original draft, Experiment, Conceptualization.

Chenghua Long: Experiment. **Kartik Chandran**: Resources, Supervision.

Declaration of Competing Interest

The authors declare that they have no known competing financial interests or personal relationships that could have appeared to influence the work reported in this paper.

Acknowledgements

This research was funded by National Science Fundation project (NSF 1706726) from US and Korea Basic Science Institute (C140310) from South Korea.

References

Ahn, J.H., Yu, R., Chandran, K., 2008. Distinctive microbial ecology and biokinetics of autotrophic ammonia and nitrite oxidation in a partial nitrification bioreactor. Biotechnol. Bioeng. 100 (6), 1078–1087.
Anbumani, S., Kakkar, P., 2018. Ecotoxicological effects of microplastics on biota: a review. Environ. Sci. Pollut. Res. Int. 25 (15), 14373–14396.
Batel, A., Linti, F., Scherer, M., Erdinger, L., Braunbeck, T., 2016. Transfer of benzo[a] pyrene from microplastics to Artemia nauplii and further to zebrafish via a trophic food web experiment: CYP1A induction and visual tracking of persistent organic pollutants. Environ. Toxicol. Chem. 35 (7), 1656–1666.
Cole, M., Lindeque, P., Halsband, C., Galloway, T.S., 2011. Microplastics as contaminants in the marine environment: a review. Mar. Pollut. Bull. 62 (12), 2588–2597.
Cole, M., Lindeque, P., Fileman, E., Halsband, C., Goodhead, R., Moger, J., Galloway, T. S., 2013. Microplastic Ingestion by Zooplankton. Environ. Sci. Technol. 47 (12), 6646–6655.
Fu, S.-F., Ding, J.-N., Zhang, Y., Li, Y.-F., Zhu, R., Yuan, X.-Z., Zou, H., 2018. Exposure to polystyrene nanoplastic leads to inhibition of anaerobic digestion system. Sci. Total Environ. 625, 64–70.
Gerdes, Z., Hermann, M., Ogonowski, M., Gorokhova, E., 2019. A novel method for assessing microplastic effect in suspension through mixing test and reference materials. Sci. Rep. 9, 10695.
Gray, A.D., Weinstein, J.E., 2017. Size- and shape-dependent effects of microplastic particles on adult daggerblade grass shrimp (Palaemonetes pugio). Environ. Toxicol. Chem. 36 (11), 3074–3080.
He, Y., Li, L., Song, K., Liu, Q., Li, Z., Xie, F., Zhao, X., 2021. Effect of microplastic particle size to the nutrients removal in activated sludge system. Mar. Pollut. Bull. 163, 111972.
Hierl, F., Wu, H.C., Westphal, H., 2021. Scleractinian corals incorporate microplastic particles: identification from a laboratory study. Environ. Sci. Pollut. Res. 28, 37882–37893.
Hwang, J., Choi, D., Han, S., Jung, S.Y., Choi, J., Hong, J., 2020. Potential toxicity of polystyrene microplastic particles. Sci. Rep. 10, 7391.
Jeon, S., Clavadetscher, J., Lee, D.-K., Chankeshwara, S.V., Bradley, M., Cho, W.-S., 2018. Surface charge-dependent cellular uptake of polystyrene nanoparticles. Nanomaterials 8 (12), 1028.
Kapoor, V., Elk, M., Li, X., Santo Domingo, J.W., 2016. Inhibitory effect of cyanide on wastewater nitrification determined using SOUR and RNA-based gene-specific assays. Lett. Appl. Microbiol. 63 (2), 155–161.
Kim, S., Marion, M., Jeong, B.-H., Hoek, E.M., 2006. Crossflow membrane filtration of interacting nanoparticle suspensions. J. Membr. Sci. 284 (1–2), 361–372.
Kim, Y.M., Park, D., Lee, D.S., Park, J.M., 2008. Inhibitory effects of toxic compounds on nitrification process for cokes wastewater treatment. J. Hazard. Mater. 152 (3), 915–921.
Kim, Y.M., Park, H., Chandran, K., 2016. Nitrification inhibition by hexavalent chromium Cr(VI)-Microbial ecology, gene expression and off-gas emissions. Water Res. 92, 254–261.
Kloet, S.K., Walczak, A.P., Louisse, J., van den Berg, H.H., Bouwmeester, H., Tromp, P., Fokkink, R.G., Rietjens, I.M., 2015. Translocation of positively and negatively charged polystyrene nanoparticles in an in vitro placental model. Toxicol. Vitr. 29 (7), 1701–1710.
Law, K.L., Thompson, R.C., 2014. Microplastics in the seas. Science 345 (6193), 144–145.
Lee, W.S., Cho, H.-J., Kim, E., Huh, Y.H., Kim, H.-J., Kim, B., Kang, T., Lee, J.-S., Jeong, J., 2019. Bioaccumulation of polystyrene nanoplastics and their effect on the toxicity of Au ions in zebrafish embryos. Nanoscale 11 (7), 3173–3185.
Lehtiniemi, M., Hartikainen, S., Näkki, P., Engström-Öst, J., Koistinen, A., Setälä, O., 2018. Size matters more than shape: Ingestion of primary and secondary microplastics by small predators. Food Web 17, e00097.
Li, L., Song, K., Yeerken, S., Geng, S., Liu, D., Dai, Z., Xie, F., Zhou, X., Wang, Q., 2020. Effect evaluation of microplastics on activated sludge nitrification and denitrification. Sci. Total Environ. 707, 135953.
Li, X., Mei, Q., Chen, L., Zhang, H., Dong, B., Dai, X., He, C., Zhou, J., 2019. Enhancement in adsorption potential of microplastics in sewage sludge for metal pollutants after the wastewater treatment process. Water Res. 157, 228–237.
Lithner, D., Larsson, Å., Dave, G., 2011. Environmental and health hazard ranking and assessment of plastic polymers based on chemical composition. Sci. Total Environ. 409 (18), 3309–3324.
Liu, H., Zhou, X., Ding, W., Zhang, Z., Nghiem, L.D., Sun, J., Wang, Q., 2019. Do microplastics affect biological wastewater treatment performance? Implications from bacterial activity experiments. ACS Sustain. Chem. Eng. 7 (24), 20097–20101.
Lundqvist, M., Stigler, J., Elia, G., Lynch, I., Cedervall, T., Dawson, K.A., 2008. Nanoparticle size and surface properties determine the protein corona with possible implications for biological impacts. PNAS 105 (38), 14265–14270.
Moghadam, B.Y., Hou, W.-C., Corredor, C., Westerhoff, P., Posner, J.D., 2012. Role of nanoparticle surface functionality in the disruption of model cell membranes. Langmuir 28 (47), 16318–16326.
Nguyen, B., Claveau-Mallet, D., Hernandez, L.M., Xu, E.G., Farner, J.M., Tufenkji, N., 2019. Separation and analysis of microplastics and nanoplastics in complex environmental samples. Acc. Chem. Res. 52 (4), 858–866.
Rehse, S., Kloas, W., Zarfl, C., 2016. Short-term exposure with high concentrations of pristine microplastic particles leads to immobilisation of Daphnia magna. Chemosphere 153, 91–99.
Rocha-Santos, T., Duarte, A.C., 2015. A critical overview of the analytical approaches to the occurrence, the fate and the behavior of microplastics in the environment. TrAC Trends Anal. Chem. 65, 47–53.
Romera-Castillo, C., Pinto, M., Langer, T.M., Álvarez-Salgado, X.A., Herndl, G.J., 2018. Dissolved organic carbon leaching from plastics stimulates microbial activity in the ocean. Nat. Commun. 9, 1430.
Rossi, G., Barnoud, J., Monticelli, L., 2014. Polystyrene nanoparticles perturb lipid membranes. J. Phys. Chem. Lett. 5 (1), 241–246.
Rotthauwe, J.-H., Witzel, K.-P., Liesack, W., 1997. The ammonia monooxygenase structural gene amoA as a functional marker: molecular fine-scale analysis of natural ammonia-oxidizing populations. Appl. Environ. Microbiol. 63 (12), 4704–4712.
Schabikowski, M., Niżnik, A., Kata, D., Graule, T., 2018. The adsorption of polystyrene nanoparticles on selected commercially available fibers: a streaming potential study. Text. Res. J. 88 (24), 2841–2853.
Seeley, M.E., Song, B., Passie, R., Hale, R.C., 2020. Microplastics affect sedimentary microbial communities and nitrogen cycling. Nat. Commun. 11, 2372.
Su, T.-C., Sathyamoorthy, S., Chandran, K., 2019. Bioaugmented methanol production using ammonia oxidizing bacteria in a continuous flow process. Bioresour. Technol. 279, 101–107.
Song, K., Li, Z., Liu, D., Li, L., 2020. Analysis of the Partial Nitrification Process Affected by Polyvinylchloride Microplastics in Treating High-Ammonia Anaerobic Digestates. ACS omega 5 (37), 23836–23842.
Sun, J., Dai, X., Wang, Q., van Loosdrecht, M.C.M., Ni, B.-J., 2019. Microplastics in wastewater treatment plants: detection, occurrence and removal. Water Res. 152, 21–37.
Sun, X., Chen, B., Li, Q., Liu, N., Xia, B., Zhu, L., Qu, K., 2018. Toxicities of polystyrene nano-and microplastics toward marine bacterium Halomonas alkaliphila. Sci. Total Environ. 642, 1378–1385.
Wang, J., Tan, Z., Peng, J., Qiu, Q., Li, M., 2016. The behaviors of microplastics in the marine environment. Mar. Environ. Res. 113, 7–17.
Wang, Z., Gao, J., Li, D., Dai, H., Zhao, Y., 2020. Co-occurrence of microplastics and triclosan inhibited nitrification function and enriched antibiotic resistance genes in nitrifying sludge. J. Hazard. Mater. 399, 123049.